



## OPEN Dosimetric and radiobiological benefits of patient-specific respiratory motion management for liver tumor stereotactic body radiotherapy

Zhenhang Xu<sup>1,2,5</sup>, Jiaxiang Gao<sup>1,2,5</sup>, Te Xu<sup>2,5</sup>, Haihua Lei<sup>1,2</sup>, Qianhong Chen<sup>3</sup>, Jiangshan Li<sup>1,2</sup>, Miaoyun Huang<sup>1,2</sup>, Xiaodong Wu<sup>1,4</sup>✉ & Yuangui Chen<sup>1,2</sup>✉

Respiratory motion management was crucial importance in radiotherapy. Our study aimed to explore the dosimetric and radiobiological benefits of various respiratory motion management strategies in liver tumor patients undergoing stereotactic body radiotherapy (SBRT). Respiratory motion images of 23 liver tumor patients were obtained by 4DCT scan under abdominal compression (AC) and free-breathing (FB). Group A included all 23 patients, while group B focused on 11 patients with tumors < 5 cm in diameter. Dosimetric and radiobiological parameters were recorded and compared across three treatment plans for each patient: Plan<sub>FB</sub>, Plan<sub>AC</sub> and Plan<sub>GAT(Respiratory gating)</sub>. For dosimetric parameters, compared to Plan<sub>AC</sub>, Plan<sub>GAT</sub> further significantly reduced liver  $D_{mean, V_{d<21.5 Gy}, V_{10Gy}}$ ; right kidney  $D_{mean}$ ; duodenum  $D_{mean, D_{0.5cc, 1cc, 5cc, 10cc}}$ ; intestine  $D_{mean, D_{0.5cc, 5cc, 10cc}}$ ; stomach  $D_{mean}$  and spinal cord  $D_{mean, V_{5Gy}}$  in group A; however, in Group B, Plan<sub>GAT</sub> only showed significant reductions in liver  $D_{mean}$  and duodenum  $D_{mean, D_{5cc, 10cc}}$ . In terms of radiobiology, compared with Plan<sub>FB</sub>, Plan<sub>AC</sub> significantly reduced liver NTCP ( $p=0.033$ ) in Group B, whereas no difference was observed in Group A ( $p=0.231$ ). Additionally, compared to Plan<sub>AC</sub>, Plan<sub>GAT</sub> further reduced liver NTCP ( $p=0.001$ ), liver EUD ( $p<0.001$ ) and right kidney EUD ( $p<0.001$ ) in Group A; however, in Group B, Plan<sub>GAT</sub> did not significantly decrease liver NTCP ( $p=0.136$ ), indicating that AC offers comparable benefits to GAT. The Pearson's correlations between the reductions in dosimetric and radiobiological parameters and tumor motion or target volume were stronger in Group B than in Group A under AC. So, GAT provides the greatest dosimetric and radiobiological benefits for liver tumors treated with SBRT, while AC offers comparable benefits for liver tumors with < 5 cm in diameter. Thus, given its technical simplicity, AC is recommended for liver tumors < 5 cm in diameter undergoing SBRT.

**Keywords** Stereotactic body radiotherapy, Respiratory motion management strategies, 4DCT, Dosimetry, NTCP

In 2022, primary liver cancer accounted for approximately 865,000 new cases and 757,000 deaths worldwide, making it the sixth most common cancer and the third leading cause of cancer death<sup>1</sup>. Additionally, the liver is a common site for metastasis from other cancers<sup>2</sup>. Unfortunately, over 70% of liver tumor patients are unsuitable for surgery<sup>3</sup>. Radiofrequency ablation (RFA) is also limited in cases where tumors are near major blood vessels, bile ducts, or the subdiaphragm<sup>4</sup>. Consequently, radiotherapy (RT) has emerged as a promising, non-invasive treatment for liver tumors due to their sensitivity to radiation. Stereotactic body radiation therapy (SBRT) delivers a high focused radiation dose to eradicate tumor cells while minimizing the risk of radiation therapy-

<sup>1</sup>Department of Radiation Oncology/Fujian Key Laboratory of Intelligent Imaging and Precision Radiotherapy for Tumors/Clinical Research Center for Radiology and Radiotherapy of Fujian Province (Digestive, Hematological and Breast Malignancies), Fujian Medical University Union Hospital, Fuzhou 350001, China. <sup>2</sup>The School of Medical imaging, Fujian Medical University, Fuzhou 350004, China. <sup>3</sup>School Sino-US Program, Fuzhou No.8, Fuzhou 350201, China. <sup>4</sup>Executive Medical Physics Associates, Miami, FL 33179, USA. <sup>5</sup>Zhenhang Xu, Jiaxiang Gao and Te Xu contributed equally to this work. ✉email: drxiaodongwu@yahoo.com; 2000cyg@fjmu.edu.cn

related complications, such as bleeding and nausea<sup>5,6</sup>. Studies have confirmed that SBRT is an effective treatment option, achieving high local control rate for inoperable early-stage primary liver cancer and oligometastasis<sup>7–9</sup>.

However, liver tumor motion caused by respiration, which can reach up to 30 mm<sup>10</sup> presents a significant challenge for SBRT. Large margins around the gross tumor volume (GTV) are often required to ensure adequate dose coverage, which increases the exposure of normal tissue to high radiation dose<sup>11</sup>. The fundamental principle of SBRT is to minimize irradiation of normal liver tissue while protecting organs at risk (OARs) and delivering an optimal dose to the tumor. Managing liver motion is critical for reducing margins, sparing normal tissue, and elevating the prescribed tumor dose<sup>12</sup>.

Common respiratory motion management strategies include active breath-holding (BH), abdominal compression (AC), and respiratory gating (GAT). The choice of an optimal strategy depends on equipment availability, staff expertise, and patient comfort and compliance. However, approximately 32% of patients undergoing SBRT are ineligible for BH<sup>13</sup>. Real-time tracking is only possible with advanced CyberKnife (CK) Synchrony system<sup>14</sup>. AC is a straightforward approach that reduces respiration motion to less than 5 mm by applying abdominal pressure, making it suitable for patients without specialized respiratory training<sup>15–17</sup>. GAT, on the other hand, uses stable and reproducible phases of the respiratory cycle to treat tumors with more comfort than BH<sup>18</sup>. Previous studies have reported the significant dosimetric advantages of GAT in liver radiotherapy, including reducing normal tissue complication probability (NTCP)<sup>19</sup>. As a result, AC and GAT are currently the most prevailing consideration for liver SBRT<sup>20</sup>.

However, prior studies have primarily focused on the benefits of AC from the perspective of motion amplitude and target volume<sup>21,22</sup> with limited analysis of its dosimetry and radiobiology advantages. Whether the tumor motion and target volume reduction achieved with AC translate into clinical benefits remains unclear. Additionally, while GAT offers dosimetric advantages, it uses only a few respiratory phases, leaving residual tumor motion and significantly increasing treatment time<sup>13,19</sup>. In contrast, AC substantially reduces motion without prolonging treatment time<sup>13</sup>. A direct comparison of GAT and AC for liver tumor patients with SBRT has not been thoroughly investigated.

This study aimed to evaluate the benefits of AC in liver tumor with SBRT using 4DCT, focusing on tumor motion amplitude, target volume, dosimetry and radiobiology. Additionally, we assessed whether AC could provide benefits similar to GAT, offering insights into its clinical applicability.

## Materials and methods

### Patient characteristics

This study prospectively included 23 consecutive patients with liver tumor treated with SBRT between February 2023 and February 2024 at our institution. Due to the retrospective nature of the study, the Ethics Committee of Fujian Medical University Union Hospital waived the need to obtain informed consent. All study protocols were approved and carried out in accordance with the institutional guidelines and regulations of Fujian Medical University Union Hospital (NO.2024ky017). The basic clinical characteristics of the patients are summarized in Table 1.

Variables	Value (n = 23)
Age (years)	
< 60	7 (30.4%)
> 60	16 (69.6%)
Gender	
Male	16 (69.6%)
Female	7 (30.4%)
Tumor Diameter (cm)	
< 5	14 (60.9%)
≥ 5	9 (39.1%)
Number of Tumors (n)	
1	19 (82.6%)
> 1	4 (17.4%)
Diagnosis	
Primary liver cancer	15 (65.2%)
Liver metastases	8 (30.4%)
Cholangiocarcinoma	1 (4.3%)
Interventional operation	
Yes	14 (60.7%)
No	9 (39.1%)

**Table 1.** Baseline clinical characteristics.

### Abdominal compression

Radiation oncologists conducted a one-minute shallow breathing training session for each patient to help them adapt to the AC device. Compression was applied during the end-expiratory phase, with the device positioned approximately 3 to 4 cm below the xiphoid process<sup>23</sup>. Patients were closely monitored to ensure a transition from abdominal to thoracic respiration until their maximum tolerance was reached.

### 4DCT data acquisition

The patients were positioned supine and immobilized using thermoplastic film and a multifunctional integrated frame. Each patient underwent two 4DCT scans using a CT simulator (Brilliance CT Big Bore, Philips, The Netherlands) with a slice thickness of 3 mm. The first 4DCT scan was performed with AC applied. Subsequently, the compression was removed, and a second 4DCT scan was conducted under the same procedure and conditions once the patient's respiratory pattern stabilized. The scanning area extended from 3 cm above the diaphragm to the iliac crest. Respiratory cycle signals were monitored using an optical body surface tracking system (C-RAD Sentinel 4DCT, Sweden). A retrospective 4DCT scanning method was used, and motion trajectory signals were converted into respiratory motion information integrated into the 4DCT image data. Each respiratory cycle was divided into 10 phases, labeled from 0 to 90%, where 50% corresponded to the end-expiratory phase and 0% to the end-inspiratory phase.

### Delineation of target volumes

The 4DCT images of each patient were transferred to the Varian treatment plan system (Varian, Eclipse V15.6, USA). Organ at risk (OAR) across all phases were initially contoured using the MANTEIA automatic outlining system. GTVs were manually contoured by the same radiation oncologist and reviewed by a senior radiation oncologist, with magnetic resonance images (MRI) and other imaging studies assisting in accurate delineation. The internal target volume (ITV) was derived using 4DCT, as recommended by the International Commission on Radiation Units and Measurements (ICRU) 83 report<sup>24</sup>. The free-breathing internal target volume (ITV<sub>FB</sub>) and abdominal compression internal target volume (ITV<sub>AC</sub>) were created by fusing the GTVs from 10 respiratory phases under respective conditions. The respiratory gating internal target volume (ITV<sub>GAT</sub>) was derived from the 40–60% respiratory phases<sup>19</sup>. Planned target volumes (PTV<sub>s</sub>) were generated by adding a uniform 3 mm margins to each ITV: PTV<sub>AC</sub> for ITV<sub>AC</sub>, PTV<sub>GAT</sub> for ITV<sub>GAT</sub> and PTV<sub>FB</sub> for ITV<sub>FB</sub><sup>25</sup>.

### Evaluation of tumor

The tumors in the ten respiratory phases generated corresponding centroid coordinate points ( $P_x$ ,  $P_y$ , and  $P_z$ ). The maximum motion variations of the tumors were determined based on the centroid positions in the LR, AP, and SI directions. To represent the overall motion of tumors, a three-dimensional vector motion ( $V_{3D}$ ) was introduced, calculated using the following formula:

$$V_{3D} = \sqrt{LR^2 + AP^2 + SI^2} \quad (1)$$

The motion variations of the tumors in the LR, AP, SI direction, and  $V_{3D}$  were compared between the FB, AC and GAT settings.

### Treatment planning and dosimetric analysis

All treatment plans were designed and optimized on the corresponding average intensity projection (AIP) images<sup>26,27</sup>. Based on existing studies, 50 Gy delivered by 5 fractions is a commonly used prescription dose scheme for liver tumor with SBRT<sup>28–30</sup>. This study adopted the same prescription dose. For all three treatment plans, volumetric modulated arc therapy (VMAT) was used for optimization with consistent beam arrangements, dose constraints, weighting factors, and computational grids. Clinical plan acceptance criteria required at least 95% of the PTV and 99% of the GTV/ITV to receive the prescribed dose of 50 Gy. Plan normalization ensured 95% PTV coverage of the prescription dose. The OAR dose constraints adhered to the Timmerman criteria<sup>31</sup>. Dose distributions were calculated using the AAA algorithm. Differences in dose delivery to the tumors and OARs among Plan<sub>AC</sub>, Plan<sub>FB</sub> and Plan<sub>GAT</sub> were calculated and recorded. In addition, this study categorized patients into two groups: Group A included all 23 patients, while group B included 11 patients with tumors < 5 cm in diameter.

### Calculation of EUD and NTCP

Dose-volume histograms (DVH) of OARs were generated from the three plans. With the dose converted to EQD2 based on the LQ model, the EUD was calculated using an effective dose reduction scheme as follows<sup>32–34</sup>:

$$EUD = \left( \sum_i (V_i D_i^a) \right)^{\frac{1}{a}} \quad (2)$$

Where  $V_i$  is the fraction of the target volume irradiated by a dose  $D_i$ , and  $a$  is a unitless model parameter specific to the tissue or tumor under evaluation. The normal tissue complication probability (NTCP) was calculated based on the EUD using the following formula<sup>33</sup>.

$$NTCP = \frac{1}{1 + \left( \frac{TD_{50}}{EUD} \right)^{4\gamma_{50}}} \quad (3)$$

Where  $TD_{50}$  represents the dose tolerance for a 50% complication rate for the normal tissue within a specific time interval, and  $\gamma_{50}$  is a parameter standing for the slope of the dose-response curve. The parameters used for different tissues are as follows (36–39):

Liver:  $a = 3$ ,  $TD_{50} = 40$  Gy,  $\gamma_{50} = 3$ ; Kidney:  $a = 1$ ,  $TD_{50} = 28$  Gy,  $\gamma_{50} = 3$ ; Duodenum:  $a = 6$ ,  $TD_{50} = 41$  Gy,  $\gamma_{50} = 4$ ; Small intestine:  $a = 6$ ,  $TD_{50} = 55$  Gy,  $\gamma_{50} = 4$ ; Spinal cord:  $a = 13$ ,  $TD_{50} = 66.5$  Gy,  $\gamma_{50} = 4$ ; Stomach:  $a = 6$ ,  $TD_{50} = 59$  Gy,  $\gamma_{50} = 4$ <sup>35–38</sup>. These calculations provided a comprehensive analysis of dosimetric and radiobiological differences among the three plans.

### Statistical analysis

All data were presented as mean  $\pm$  standard deviation (SD). For data with a normal distribution and homogeneity of variance, overall statistical differences were assessed using two-way ANOVA, followed by multiple comparisons using the least significant difference (LSD) test. For data that did not conform to these assumptions, comparisons were conducted using Friedman's M test, followed by multiple comparisons with the q test and Bonferroni correction. Pearson's correlation was calculated to evaluate the relationship between parameter reductions. Statistical analyses were performed using SPSS 27.0 software, and a  $p$ -value  $< 0.05$  was considered statistically significant.

### Results

Tumor motion and target volume in the AC and GAT groups were significantly reduced compared to FB. Tumor motion was found to be anisotropic, especially in the SI direction, showing much greater displacement than the LR and AP directions ( $p < 0.001$ ). The tumor motion and target volume parameters are illustrated in Fig. 1. The average tumor motion in  $V_{3D}$  was  $9.45 \pm 3.28$  mm,  $6.40 \pm 3.34$  mm and  $2.15 \pm 1.44$  mm in the FB, AC and GAT groups, respectively ( $p < 0.001$ ). With the application of AC, tumor motion exceeding 10 mm was reduced to 4 cases (12.5%), and motion exceeding 5 mm was reduced to 16 cases (50%). Motion in the SI direction increased in only 2 tumors (6.3%), while the remaining 30 tumors (93.8%) showed varying degrees of reduction. Among these, 13 tumors (40.6%) showed a reduction of more than 3 mm. Displacement in the AP direction decreased in 24 tumors (75%). Tumor motion in the AP and SI directions decreased by 30.0% and 32.8% ( $p = 0.026$ ,  $p < 0.001$ , respectively); while  $V_{3D}$  was reduced by 32.3% ( $p < 0.001$ ). Compared to AC, GAT further reduced tumor motion in the LR, AP, and SI directions ( $p < 0.001$ ,  $p = 0.026$ ,  $p = 0.008$ , respectively) and demonstrate an additional reduction in  $V_{3D}$  ( $p = 0.026$ ).  $ITV_{AC}$  and  $ITV_{GAT}$  were significantly smaller than  $ITV_{FB}$  ( $p < 0.001$ ). Further pairwise comparison revealed that  $ITV_{GAT}$  was also significantly smaller than  $ITV_{AC}$  ( $p = 0.012$ ). Similar results were observed for PTV, mirroring the trends seen in ITV (Fig. 1B).

Dose parameters comparison for OARs among  $Plan_{FB}$ ,  $Plan_{AC}$ , and  $Plan_{GAT}$  are presented in Tables 2 and 3. Compared to FB,  $Plan_{AC}$  significantly reduced liver  $D_{mean}$  ( $p < 0.001$ ),  $V_{d < 21.5 \text{ Gy}}$  ( $p < 0.001$ ),  $V_{10 \text{ Gy}}$  ( $p = 0.002$ ), stomach  $D_{50cc}$  ( $p = 0.030$ ) and spinal cord  $D_{mean}$  ( $p = 0.019$ ),  $D_{0.1cc}$  ( $p = 0.041$ ),  $D_{1cc}$  ( $p = 0.037$ ) in Group A. In Group B,  $Plan_{AC}$  also reduced liver  $D_{mean}$  ( $p < 0.018$ ),  $V_{d < 21.5 \text{ Gy}}$  ( $p < 0.012$ ),  $V_{10 \text{ Gy}}$  ( $p = 0.036$ ), as well as spinal cord  $D_{mean}$  ( $p = 0.029$ ),  $D_{0.1cc}$  ( $p = 0.007$ ),  $D_{1cc}$  ( $p = 0.018$ ). For GAT vs. FB,  $Plan_{GAT}$  significantly reduced most OAR dose indicators ( $p < 0.05$ ) except for spinal cord  $D_{0.1cc}$  ( $p = 0.186$ ) and  $D_{1cc}$  ( $p = 0.137$ ) in Group (A)  $Plan_{GAT}$  also significantly reduced massive parameters except for left kidney  $D_{mean}$  ( $p = 0.057$ ), stomach  $D_{50cc}$  ( $p = 0.066$ ), spinal cord  $D_{0.1cc}$  ( $p = 0.070$ ) and  $D_{1cc}$  ( $p = 0.125$ ) In Group (B) As regards GAT vs. AC,  $Plan_{GAT}$  significantly reduced OAR dose indicators in Group A, including liver  $D_{mean}$  ( $p < 0.001$ ),  $V_{d < 21.5 \text{ Gy}}$  ( $p = 0.003$ ),  $V_{10 \text{ Gy}}$  ( $p = 0.030$ ), right kidney  $D_{mean}$  ( $p = 0.005$ ), duodenum  $D_{mean}$  ( $p = 0.004$ ),  $D_{0.5cc}$  ( $p = 0.006$ ),  $D_{1cc}$  ( $p = 0.006$ ),

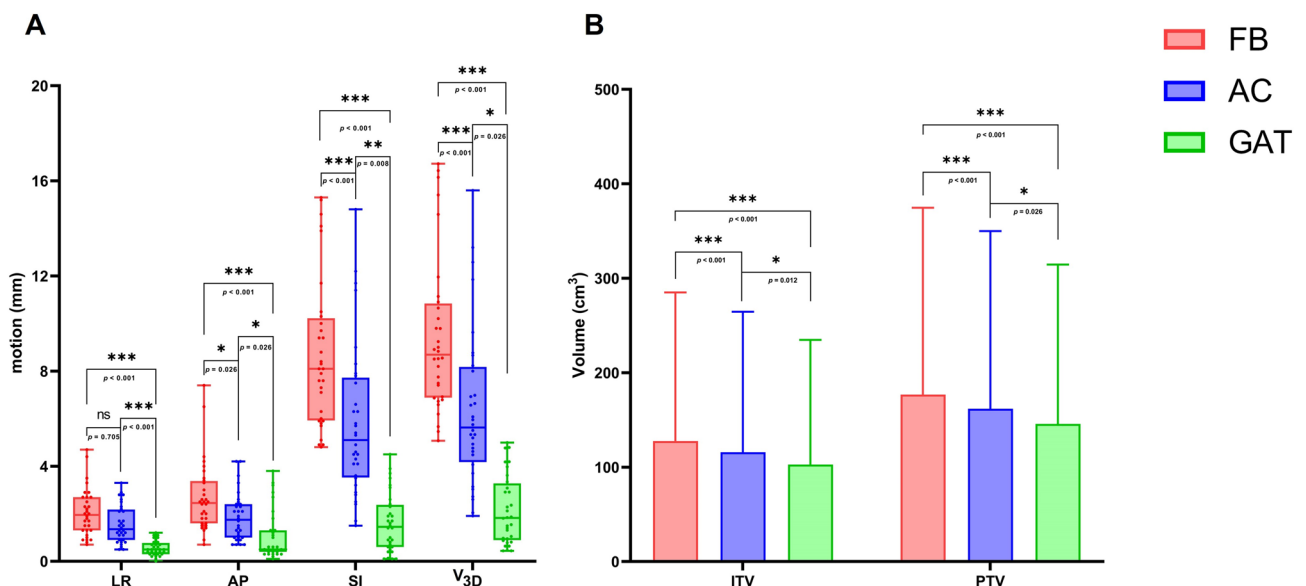


**Fig. 1.** Comparisons of tumor motion, ITV and PTV under different motion management strategies.

Index	Plan <sub>FB</sub>	Plan <sub>AC</sub>	Plan <sub>GAT</sub>	p-value			
				Overall	a vs. b	a vs. c	b vs. c
liver D <sub>mean</sub> (Gy)	14.44 ± 6.96	13.76 ± 6.85	13.08 ± 6.77	<0.001	<0.001	<0.001	<0.001
liver V <sub>d&lt;21.5 Gy</sub> (cc)	799.54 ± 305.37	829.83 ± 298.11	849.60 ± 285.82	<0.001	<0.001	<0.001	0.003
liver V <sub>10 Gy</sub> (%)	56.20 ± 29.09	53.37 ± 28.93	51.47 ± 28.76	<0.001	0.002	<0.001	0.030
left kidney D <sub>mean</sub> (Gy)	2.12 ± 2.86	1.85 ± 2.46	1.67 ± 2.30	<0.001	0.166	<0.001	0.098
right kidney D <sub>mean</sub> (Gy)	4.78 ± 5.34	4.49 ± 5.31	3.18 ± 3.89	<0.001	0.196	<0.001	0.005
duodenum D <sub>mean</sub> (Gy)	4.08 ± 5.08	3.77 ± 5.42	2.99 ± 4.15	<0.001	0.421	<0.001	0.004
duodenum D <sub>0.5 cc</sub> (Gy)	13.88 ± 13.40	13.23 ± 12.21	10.73 ± 11.03	<0.001	1.000	<0.001	0.006
duodenum D <sub>1cc</sub> (Gy)	12.75 ± 12.55	11.94 ± 11.39	9.84 ± 10.35	<0.001	1.000	0.002	0.006
duodenum D <sub>5cc</sub> (Gy)	8.33 ± 9.01	7.84 ± 9.20	6.59 ± 8.74	<0.001	1.000	<0.001	0.001
duodenum D <sub>10cc</sub> (Gy)	6.13 ± 7.99	5.84 ± 8.10	4.93 ± 7.75	<0.001	1.000	<0.001	0.003
intestine D <sub>mean</sub> (Gy)	1.92 ± 3.37	1.69 ± 2.89	1.39 ± 2.58	<0.001	0.231	<0.001	0.003
intestine D <sub>0.5 cc</sub> (Gy)	13.95 ± 14.10	11.18 ± 11.93	8.83 ± 9.12	<0.001	0.081	<0.001	0.024
intestine D <sub>5cc</sub> (Gy)	10.07 ± 10.71	8.56 ± 10.85	6.23 ± 6.77	<0.001	0.140	<0.001	0.006
intestine D <sub>10cc</sub> (Gy)	8.05 ± 9.40	7.63 ± 10.34	5.45 ± 6.11	<0.001	0.196	<0.001	0.005
stomach D <sub>mean</sub> (Gy)	7.23 ± 6.01	7.00 ± 5.95	6.07 ± 5.16	<0.001	0.715	<0.001	0.002
stomach D <sub>0.5 cc</sub> (Gy)	18.18 ± 13.86	17.51 ± 13.34	15.49 ± 11.75	0.002	0.906	0.002	0.055
stomach D <sub>5cc</sub> (Gy)	14.86 ± 12.28	14.22 ± 11.63	13.09 ± 10.41	0.003	0.421	0.002	0.166
stomach D <sub>10cc</sub> (Gy)	13.76 ± 11.69	12.90 ± 10.65	11.92 ± 9.55	0.001	0.117	0.001	0.314
stomach D <sub>50cc</sub> (Gy)	9.59 ± 7.82	8.92 ± 7.40	8.52 ± 7.19	0.004	0.030	0.010	1.000
spinal cord D <sub>mean</sub> (Gy)	4.04 ± 2.64	3.81 ± 2.57	3.54 ± 2.38	<0.001	0.019	<0.001	0.006
spinal cord D <sub>0.1 cc</sub> (Gy)	14.73 ± 5.93	14.17 ± 5.97	14.37 ± 6.17	0.116	0.041	0.186	0.453
spinal cord D <sub>1cc</sub> (Gy)	13.63 ± 5.69	13.09 ± 5.60	13.25 ± 5.81	0.099	0.037	0.137	0.531
spinal cord V <sub>5 Gy</sub> (%)	27.92 ± 17.52	26.87 ± 16.55	24.54 ± 16.18	<0.001	0.170	<0.001	0.004

**Table 2.** Dosimetric comparison of oars among Plan<sub>FB</sub>, Plan<sub>AC</sub> and Plan<sub>GAT</sub> (group A). a: Plan<sub>FB</sub>: free breathing treatment plan; b: Plan<sub>AC</sub>: abdominal compression treatment plan; c: Plan<sub>GAT</sub>: respiratory gating treatment plan; V<sub>d<21.5 Gy</sub>: the critical normal liver volume receiving <21.5 Gy; D<sub>mean</sub>: mean dose; D<sub>0.1cc</sub>, D<sub>0.5cc</sub>, D<sub>1cc</sub>, D<sub>5cc</sub>, D<sub>10cc</sub>, D<sub>50cc</sub>: doses to the specified volume of the organ (0.1 cc, 0.5 cc, 1 cc, 5 cc, 10 cc, 50 cc); V<sub>5 Gy</sub>: V<sub>10 Gy</sub>: % of organ volume receiving specific dose (5 Gy, 10 Gy).

D<sub>5cc</sub> ( $p=0.001$ ), D<sub>10cc</sub> ( $p=0.003$ ), intestine D<sub>mean</sub> ( $p=0.003$ ), D<sub>0.5cc</sub> ( $p=0.024$ ), D<sub>5cc</sub> ( $p=0.006$ ), D<sub>10cc</sub> ( $p=0.005$ ), stomach D<sub>mean</sub> ( $p<0.002$ ) and spinal cord D<sub>mean</sub> ( $p=0.006$ ), V<sub>5Gy</sub> ( $p=0.004$ ). These results suggest that GAT was the optimal respiratory motion management method for Group A. For group B, however, GAT only reduces liver D<sub>mean</sub> ( $p=0.004$ ) and duodenum D<sub>mean</sub> ( $p=0.032$ ), D<sub>5cc</sub> ( $p=0.012$ ), D<sub>10cc</sub> ( $p=0.043$ ) compared to AC. This indicates that the benefits of GAT were less pronounced in Group B compared to Group A.

The distribution of OAR doses in Group A was more variable, with values spread across both the white (motion management effective) and gray (motion management ineffective) regions, especially for serial organs under AC (Fig. 2A and C). In contrast, OAR doses in Group B under AC were primarily located in the white region (Fig. 2B and D), indicating that AC was highly effective in this group. Under GAT, OAR doses in both Group A and Group B were predominantly located in the white region (Fig. 2), suggesting that the benefits of GAT were greater for Group A than Group B. Motion management strategies were shown to tighten the dose distribution (Fig. 3). Both Plan<sub>AC</sub> and Plan<sub>GAT</sub> significantly tightened the isodose lines, especially in the SI direction for Group B. However, for Group A, Plan<sub>GAT</sub> demonstrated a better dose distribution than Plan<sub>AC</sub>. These dose findings were indicative of the fact that AC was effective for the group B. For group A, GAT proved to be more effective, especially for serial organs.

The results of EUD and NTCP were detailed in Tables 4 and 5. For AC vs. FB, Liver EUD, intestine EUD and spinal cord EUD were significantly lower in Plan<sub>AC</sub> compared to Plan<sub>FB</sub>; Plan<sub>AC</sub> significantly reduced liver NTCP ( $p=0.033$ ) in Group B, whereas no difference was observed in Group A ( $p=0.231$ ). AC demonstrated greater radiobiological benefits in Group B than in Group A, particularly for liver NTCP. In regard to GAT vs. FB, EUD of all OARs in Plan<sub>GAT</sub> were significantly reduced compared to other plans, except for the spinal cord. Liver EUD and right kidney EUD were significantly lower with Plan<sub>GAT</sub> compared to Plan<sub>AC</sub>. For liver NTCP, there was significant difference between Plan<sub>AC</sub> and Plan<sub>GAT</sub> in Group A ( $p=0.001$ ), while no significant difference was observed in Group B ( $p=0.136$ ). Similar to Fig. 2, the radiobiological benefits of OARs were graphically illustrated in Fig. 4 using two zones: the white region representing motion management (MM) effectiveness, and the gray region representing MM ineffectiveness. As shown, under GAT, radiobiological parameters of OARs were predominately located in the white region for both Group A and Group B. However, under AC, the radiobiological parameters were mainly distributed in the white region only in Group B (Fig. 4B, D). This indicates that AC and GAT provide comparable radiobiological benefits in Group B. These findings align with the dose parameters results, further confirming that GAT offers the greatest dosimetric and radiobiological

Index	Plan <sub>FB</sub>	Plan <sub>AC</sub>	Plan <sub>GAT</sub>	p-value			
				Overall	a vs. b	a vs. c	b vs. c
liver D <sub>mean</sub> (Gy)	9.50 ± 4.68	8.80 ± 4.25	7.93 ± 4.01	< 0.001	0.018	< 0.001	0.004
liver V <sub>d&lt;21.5 Gy</sub> (cc)	944.00 ± 279.19	969.53 ± 271.90	983.77 ± 260.23	0.002	0.012	< 0.001	0.139
liver V <sub>10 Gy</sub> (%)	36.69 ± 21.55	33.79 ± 20.18	31.25 ± 20.42	0.002	0.036	< 0.001	0.063
left kidney D <sub>mean</sub> (Gy)	0.81 ± 1.10	0.78 ± 1.11	0.47 ± 0.67	0.014	1.000	0.057	0.210
right kidney D <sub>mean</sub> (Gy)	2.22 ± 2.93	1.78 ± 2.38	1.32 ± 1.96	< 0.001	0.165	0.001	0.329
duodenum D <sub>mean</sub> (Gy)	1.36 ± 1.51	1.14 ± 1.36	0.78 ± 0.74	< 0.001	0.602	< 0.001	0.032
duodenum D <sub>0.5 cc</sub> (Gy)	6.51 ± 7.42	5.44 ± 6.68	4.72 ± 5.42	0.002	0.859	0.002	0.057
duodenum D <sub>1cc</sub> (Gy)	5.74 ± 6.83	4.98 ± 6.23	4.24 ± 4.89	0.002	0.859	0.002	0.057
duodenum D <sub>5cc</sub> (Gy)	3.87 ± 4.90	3.28 ± 4.48	1.98 ± 2.40	< 0.001	0.602	< 0.001	0.012
duodenum D <sub>10cc</sub> (Gy)	2.38 ± 3.18	2.12 ± 3.16	1.02 ± 1.09	0.002	1.000	0.003	0.043
intestine D <sub>mean</sub> (Gy)	0.42 ± 0.37	0.32 ± 0.31	0.25 ± 0.22	< 0.001	0.407	0.001	0.099
intestine D <sub>0.5 cc</sub> (Gy)	8.35 ± 12.02	5.70 ± 5.86	4.86 ± 5.85	0.001	0.057	0.002	0.859
intestine D <sub>5cc</sub> (Gy)	4.75 ± 4.29	3.44 ± 2.90	2.60 ± 2.51	0.001	0.329	0.001	0.165
intestine D <sub>10cc</sub> (Gy)	3.33 ± 3.13	2.82 ± 2.77	2.24 ± 2.50	0.002	0.497	0.002	0.128
stomach D <sub>mean</sub> (Gy)	2.96 ± 2.26	2.65 ± 1.95	2.33 ± 2.22	0.038	0.602	0.032	0.602
stomach D <sub>0.5 cc</sub> (Gy)	8.36 ± 3.63	7.78 ± 3.30	7.33 ± 3.94	0.077	0.190	0.026	0.303
stomach D <sub>5cc</sub> (Gy)	6.91 ± 3.56	6.54 ± 3.11	6.03 ± 3.69	0.036	0.256	0.011	0.118
stomach D <sub>10cc</sub> (Gy)	6.22 ± 3.57	5.96 ± 3.01	5.34 ± 3.71	0.039	0.427	0.014	0.074
stomach D <sub>50cc</sub> (Gy)	4.20 ± 3.39	3.71 ± 2.76	3.44 ± 3.29	0.169	0.223	0.066	0.500
spinal cord D <sub>mean</sub> (Gy)	2.08 ± 1.29	1.86 ± 1.06	1.74 ± 1.07	0.006	0.029	0.002	0.216
spinal cord D <sub>0.1 cc</sub> (Gy)	11.07 ± 5.57	9.98 ± 4.82	10.37 ± 5.61	0.024	0.007	0.070	0.301
spinal cord D <sub>1cc</sub> (Gy)	10.02 ± 5.07	9.13 ± 4.50	9.47 ± 5.26	0.054	0.018	0.125	0.340
spinal cord V <sub>5 Gy</sub> (%)	15.53 ± 10.31	14.47 ± 8.40	12.53 ± 7.78	0.020	1.000	0.032	0.165

**Table 3.** Dosimetric comparison of oars among Plan<sub>FB</sub>, Plan<sub>AC</sub> and Plan<sub>GAT</sub> (group B). a: Plan<sub>FB</sub>: free breathing treatment plan; b: Plan<sub>AC</sub>: abdominal compression treatment plan; c: Plan<sub>GAT</sub>: respiratory gating treatment plan; V<sub>d<21.5 Gy</sub>: the critical normal liver volume receiving < 21.5 Gy; D<sub>mean</sub>: mean dose; D<sub>0.1cc</sub>, D<sub>0.5cc</sub>, D<sub>1cc</sub>, D<sub>5cc</sub>, D<sub>10cc</sub>, D<sub>50cc</sub>: doses to the specified volume of the organ (0.1 cc, 0.5 cc, 1 cc, 5 cc, 10 cc, 50 cc); V<sub>5 Gy</sub>, V<sub>10 Gy</sub>: % of organ volume receiving specific dose (5 Gy, 10 Gy).

benefits for liver tumors treated with SBRT. However, for liver tumors with a diameter < 5 cm, AC provides comparable benefits to GAT.

We further analyzed the correlations of the reduction in the parameters under AC. All correlations values in Group B were monotonically increasing, except for the correlation between intestine EUD and V<sub>3D</sub> ( $r = -0.139$ ). Strong correlations ( $r > 0.7$ ) were observed in Group B between liver D<sub>mean</sub>, V<sub>d<21.5 Gy</sub>, EUD and stomach EUD with V<sub>3D</sub>, liver V<sub>d<21.5 Gy</sub> with ITV, and liver D<sub>mean</sub>, V<sub>d<21.5 Gy</sub> with PTV (Fig. 5). However, no strong correlations were found in group A. These findings indicate that the correlations between tumor motion, target volume, and dose or radiobiological parameters were significantly stronger in group B than in group (A) This suggests that the benefits of tumor motion management benefits with AC are more clinically relevant in Group (B) Specifically, small tumors (diameter < 5 cm) derive more benefits from AC.

## Discussion

Respiratory motion management strategies can be highly effective in reducing the magnitude of tumor motion, leading to significantly reductions in target volume and sparing more normal tissue<sup>35</sup>. This reduction in normal tissue exposure decreases the radiation-induced complications probability, such as radiation-induced liver disease (RILD)<sup>36,37</sup>. The availability of multiple motion management strategies offers flexibility in clinical practice. While early studies focused on changes in the amplitude of tumor motion and target volume with AC in liver tumor SBRT<sup>21,22</sup> little attention has been given to dosimetric and radiobiological benefits. Additionally, the comparative clinical benefits between GAT and AC remain unclear. Thus, this study aimed to evaluate the effects of respiratory motion management strategies on liver tumor SBRT using 4DCT, focusing not only on tumor motion and target volume, but also on dose distribution and the expected clinical outcome based on EUD and NTCP of OARs.

Respiratory motion management strategies, including AC and GAT, have been shown to significantly reduce tumor motion amplitude. In this study, AC reduced overall tumor motion significantly ( $p < 0.001$ ), consistent with findings by Eccles et al. and Heinzerling et al.<sup>38,39</sup>. AC reduced tumor motion by 2.9 and 0.8 mm in the SI and AP directions respectively, with 40.6% of tumors exhibiting a reduction of > 3 mm in the SI direction. This reduction in tumor motion resulted in significantly decreases in ITV ( $p < 0.001$ ) and PTV ( $p < 0.001$ ). Similarly, GAT further reduced tumor motion ( $p < 0.001$ ) and resulted in reductions in ITV ( $p < 0.001$ ) and PTV ( $p < 0.001$ ) compared to FB. Compared to AC, GAT achieved additional reduction in V<sub>3D</sub> ( $p = 0.026$ ), ITV ( $p = 0.012$ ) and PTV ( $p = 0.026$ ). These results align with previous studies<sup>19,40</sup>.

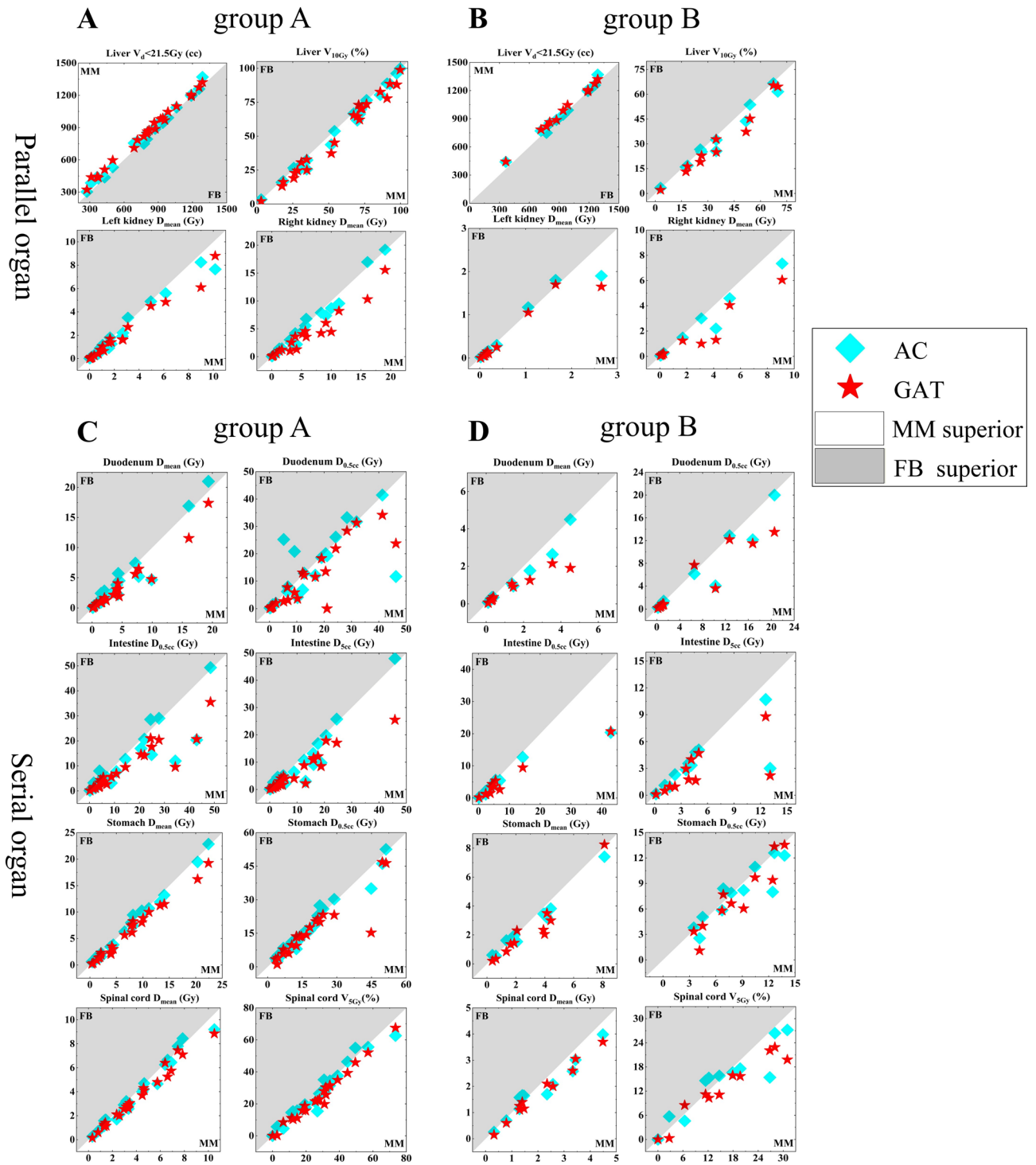


**Fig. 2.** Comparisons of the PlanFB, PlanAC and PlanGAT by the dosimetric parameters to the OARs. For every patient, each parameter is associated with three values (from PlanFB, PlanAC and PlanGAT). In each graph, for the parameter X, each patient will contribute a pair of symbols, i.e., a rhomboid and a star; the cyan rhomboid is plotted by the coordinates XFB, XAC, while the red star is plotted by XFB, XGAT. A symbol falling in the gray area implies the parameter is favorable in the PlanFB. A symbol falling in the white area implies the parameter is favorable in the MM (motion management) plan.

Focusing solely on reductions in amplitude of movement is insufficient for clinical needs. Decreasing radiation doses to normal liver tissue, kidneys, spinal cord, and intestines translate into fewer side effects and improved clinical outcomes. This study showed that AC reduced the number of patients exceeding dose limits from 6 to 3 in Group A and achieved full compliance in Group B. These dosimetric benefits of AC for liver

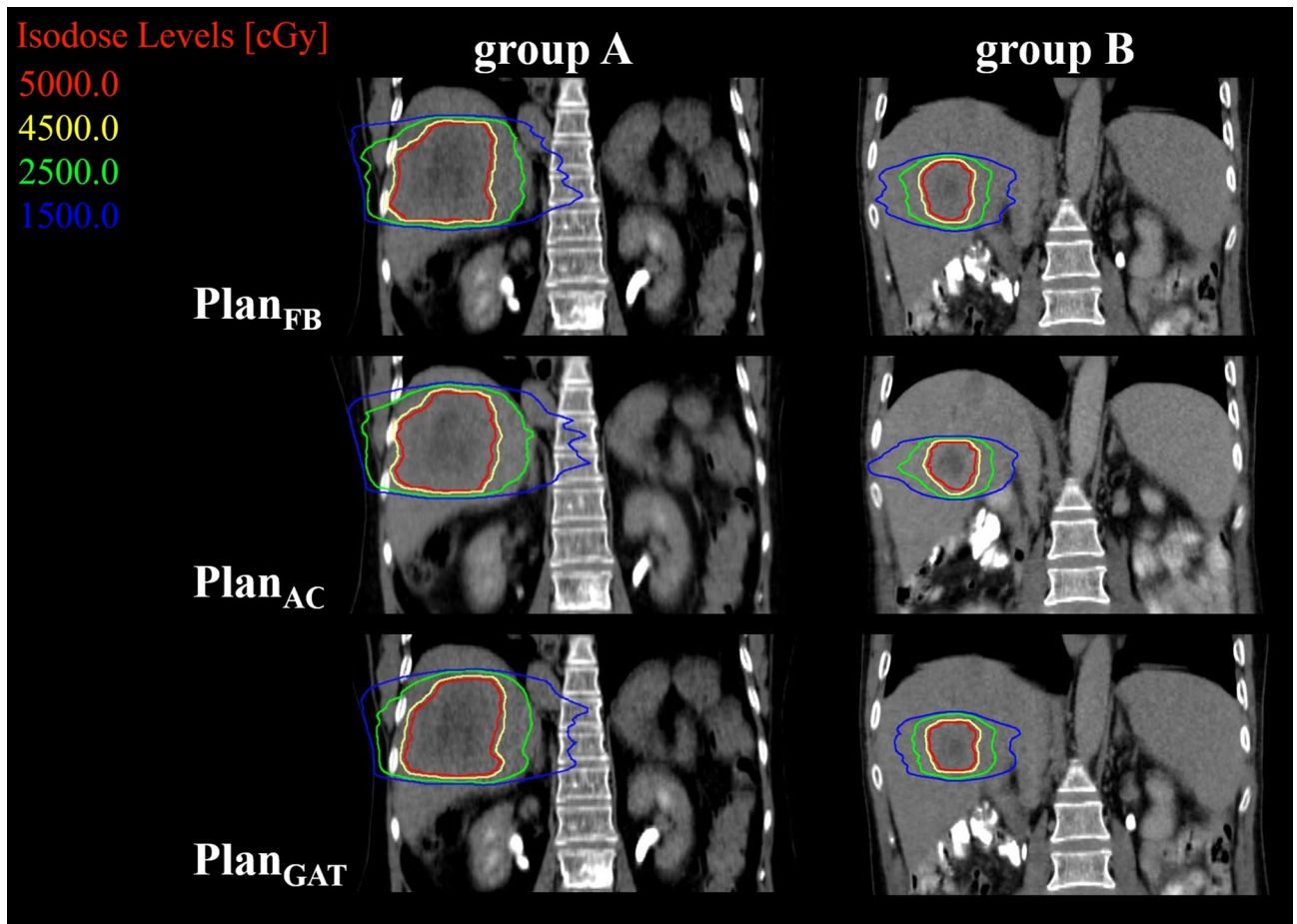


**Fig. 3.** Dose distributions among PlanFB, PlanAC and PlanGAT for a representative patient in group A and B. The 5000 cGy, 4500 cGy, 2500 cGy and 1500 cGy isodose lines are in red, yellow, green and dark blue, respectively.

Index	Plan <sub>FB</sub>	Plan <sub>AC</sub>	Plan <sub>GAT</sub>	p-value			
				Overall	a vs. b	a vs. c	b vs. c
liver EUD (Gy)	44.67 ± 12.83	43.59 ± 12.63	42.29 ± 12.58	<0.001	<0.001	<0.001	<0.001
liver NTCP (%)	66.01 ± 37.49	62.79 ± 38.14	58.16 ± 38.57	<0.001	0.231	<0.001	0.001
left kidney EUD (Gy)	1.91 ± 3.03	1.62 ± 2.47	1.45 ± 2.36	<0.001	0.030	<0.001	0.166
right kidney EUD (Gy)	7.32 ± 9.77	6.70 ± 9.60	3.94 ± 6.23	<0.001	0.906	<0.001	<0.001
duodenum EUD (Gy)	14.27 ± 18.60	12.26 ± 14.82	9.70 ± 12.32	<0.001	0.421	<0.001	0.055
intestine EUD (Gy)	9.16 ± 13.04	7.11 ± 12.24	4.88 ± 6.66	<0.001	0.015	<0.001	0.098
stomach EUD (Gy)	15.90 ± 19.21	14.79 ± 17.42	12.17 ± 14.24	<0.001	0.421	<0.001	0.055
spinal cord EUD (Gy)	14.99 ± 8.48	14.15 ± 8.35	14.51 ± 8.74	0.129	0.045	0.243	0.383

**Table 4.** Radiobiological comparison of oars among Plan<sub>FB</sub>, Plan<sub>AC</sub> and Plan<sub>GAT</sub> (group A). a: Plan<sub>FB</sub>: free breathing treatment plan; b: Plan<sub>AC</sub>: abdominal compression treatment plan; c: Plan<sub>GAT</sub>: respiratory gating treatment plan; EUD: equivalent uniform dose (Gy); NTCP: normal tissue complication probability (%).

tumor SBRT are among the highlights of this study, rarely addressed in prior research. In contrast, all patients using GAT met dose restriction criteria and reduced most OAR dose parameters, consistent with the findings of Xi et al. and Gabryś et al.<sup>19,40</sup>. Comparisons between GAT and AC showed that GAT provided superior dosimetric benefits, particularly in Group A. Both AC and GAT increased the likelihood of SBRT eligibility without excessive radiation-related complications, with GAT being more effective in Group A.

For liver,  $V_{d < 21.5 \text{ Gy}}$  (cc) is a key evaluation parameter based on the Timmerman criteria. AC and GAT significantly reduced this volume compared to FB in both groups ( $p < 0.05$ ). However, compared with AC, GAT further reduced liver  $V_{d < 21.5 \text{ Gy}}$  in Group A ( $p = 0.003$ ), while no significant difference was found in Group B

Index	Plan <sub>FB</sub>	Plan <sub>AC</sub>	Plan <sub>GAT</sub>	p-value			
				Overall	a vs. b	a vs. c	b vs. c
liver EUD (Gy)	34.43 ± 12.35	33.30 ± 11.79	32.59 ± 10.39	< 0.001	0.020	0.020	0.001
liver NTCP (%)	38.67 ± 36.21	34.00 ± 33.27	24.73 ± 25.49	< 0.001	0.033	< 0.001	0.136
left kidney EUD (Gy)	0.40 ± 0.60	0.35 ± 0.67	0.32 ± 0.43	0.017	0.859	0.017	0.264
right kidney EUD (Gy)	2.77 ± 3.72	2.02 ± 2.76	1.19 ± 2.01	< 0.001	0.859	< 0.001	0.009
duodenum EUD (Gy)	4.74 ± 5.91	2.91 ± 4.95	2.82 ± 3.46	0.003	0.264	0.002	0.264
intestine EUD (Gy)	5.27 ± 11.76	2.65 ± 4.11	2.60 ± 4.92	< 0.001	0.009	0.001	1.000
stomach EUD (Gy)	4.81 ± 2.73	4.33 ± 2.29	4.05 ± 2.76	0.026	0.079	0.008	0.290
spinal cord EUD (Gy)	9.70 ± 7.02	8.22 ± 5.75	8.99 ± 7.09	0.033	0.010	0.186	0.155

**Table 5.** Radiobiological comparison of oars among Plan<sub>FB</sub>, Plan<sub>AC</sub> and Plan<sub>GAT</sub> (group B). a: Plan<sub>FB</sub>: free breathing treatment plan; b: Plan<sub>AC</sub>: abdominal compression treatment plan; c: Plan<sub>GAT</sub>: respiratory gating treatment plan; EUD: equivalent uniform dose (Gy); NTCP: normal tissue complication probability (%).

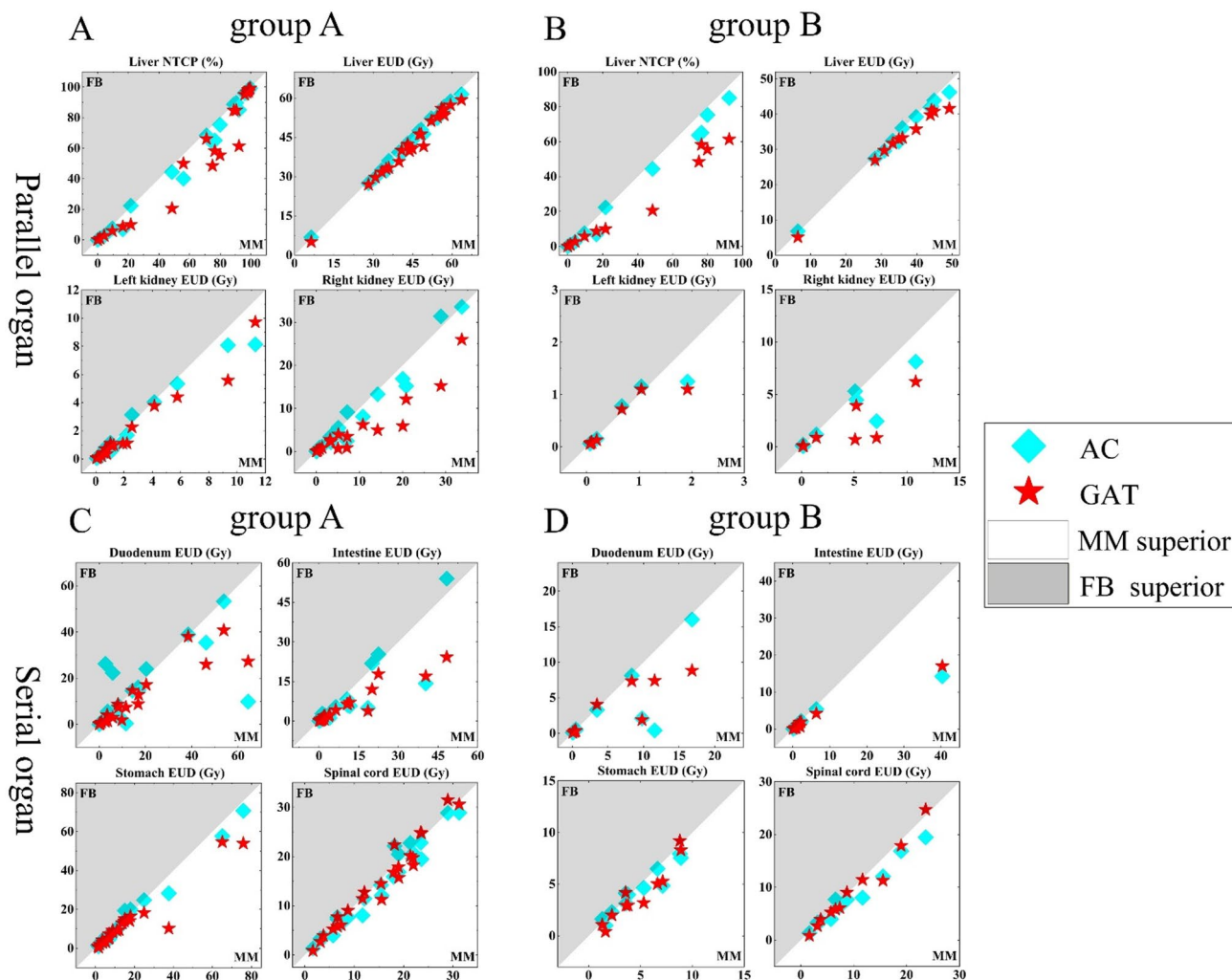


**Fig. 4.** Comparisons of the PlanFB, PlanAC and PlanGAT by the radiobiological parameters in relation to the OARs. For every patient, each parameter is associated with three values (from PlanFB, PlanAC and PlanGAT). In each graph, for the parameter X, each patient will contribute a pair of symbols, i.e., a rhomboid and a star; the cyan rhomboid is plotted by the coordinates XFB, XAC, while the red star is plotted by XFB, XGAT. A symbol falling in the gray area implies the parameter is favorable in the PlanFB, but in the white area is favorable in the MM (motion management) plan.

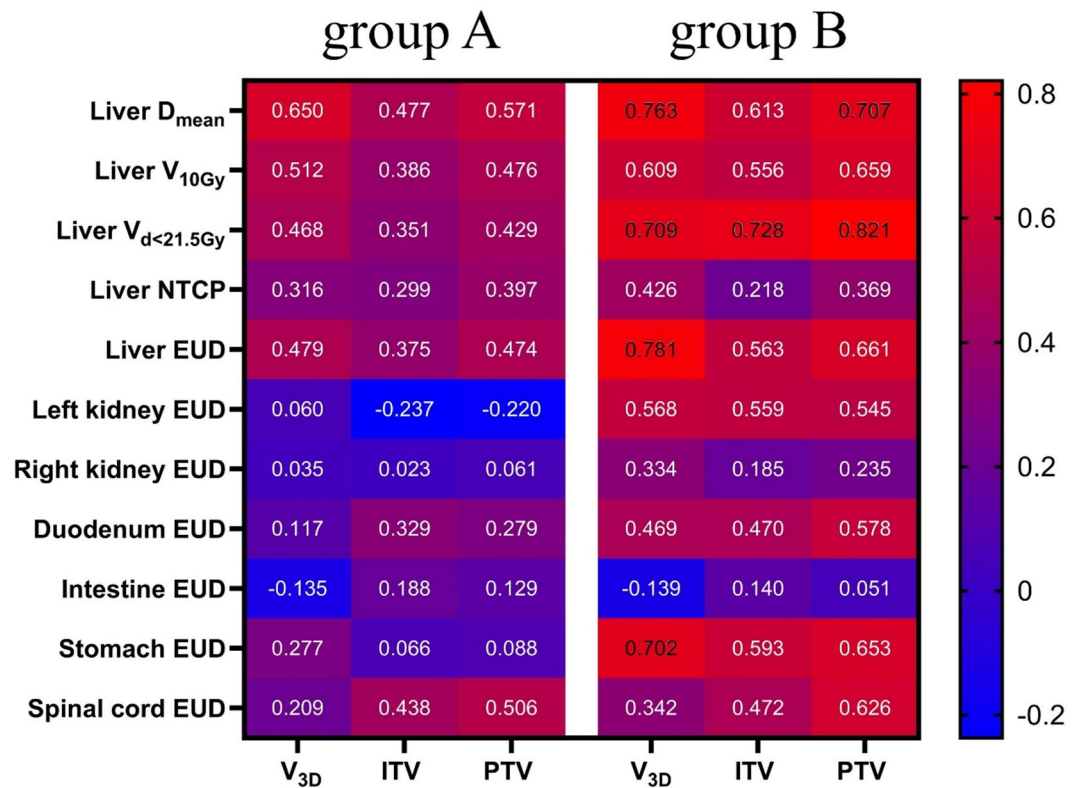


**Fig. 5.** Correlation between the dose–volume and radiobiology reduction to OARs and the reduction in V<sub>3D</sub>, ITV and PTV under AC.

( $p=0.139$ ). These findings suggest that AC works well-suited for Group B, while GAT is the optimal choice for Group A.

While dosimetric benefits focus on physical parameters, radiobiological modeling better reflects clinical outcomes due to differences in tissue radiosensitivity<sup>41–44</sup>. This study is the first to use a radiobiological model to compare EUD and NTCP of OARs between FB, AC and GAT. AC significantly reduced liver NTCP in Group B ( $p=0.033$ ) compared to FB but showed no significant difference in Group A ( $p=0.231$ ). Further comparisons revealed that GAT did not reduce liver NTCP in Group B ( $p=0.136$ ), but significantly reduced it in Group A ( $p=0.001$ ). These findings confirm that AC and GAT have the comparable benefits for Group B, while GAT is more effective for Group A.

Our study showed that AC provided greater dosimetric and radiobiological benefits in Group B than in Group A. Correlation analysis revealed stronger relationships in Group B, indicating greater benefits (Fig. 5). V<sub>3D</sub> was reduced by  $29.04 \pm 22.38\%$  and  $30.09 \pm 26.87\%$  in Group A and Group B respectively, with no statistical significance ( $p=0.906$ ), suggesting that the difference in dose reduction was not due to tumor motion amplitude. ITV and PTV were reduced by  $12.69 \pm 9.99\%$  and  $11.14 \pm 8.48\%$  in Group A, compared to  $17.22 \pm 11.82\%$  and  $15.11 \pm 10.20\%$  in Group B, with no significant differences ( $p=0.253$  for ITV,  $p=0.241$  for PTV). The greater ITV and PTV reductions in Group B, compared to no difference of V<sub>3D</sub> reductions between Group A and B, may result from Group A containing larger tumors (diameter > 5 cm). As Gargett M et al. reported, larger GTVs reduce the correlation between the PTV reduction and tumor motion<sup>12</sup>. Thus, reduced tumor motion amplitude by AC did not translate into significant dosimetric and radiobiologic benefits in Group A. AC is more suitable for Group B with small tumors (diameter < 5 cm).

The deficiency of this article lies in the fact that the high attenuation of radiation by the abdominal compression device may cause skin exposure for high-dose irradiation, it is necessary to avoid setting the radiation field in the high-density structure of the abdominal compression frame during the planning design process (such as fixed screws and frame fixed points)<sup>45</sup>. This study also found that the application of abdominal compression devices might cause irregular breathing in patients, resulting in artifacts in 4DCT images and reducing the reliability of this 4DCT scan. Therefore, each patient in this study received basic respiratory training before the 4DCT scan, and the scan range as well as the positions of the primary and secondary gated points were adjusted multiple times to perform 4DCT image acquisition during the period when the respiratory waveforms were the most regular and the fluctuations were the most obvious. Finally, the overall sample size of the experiment was relatively small and might not be able to replace the real situation of patients with liver tumors. Subsequently, the sample size will continue to be increased to improve the reliability of the study.

## Conclusions

Respiratory motion management strategies have capability to achieve significant reductions in liver tumor motion, target volume, and clinically advantageous dosimetric and radiobiological values of OARs. GAT provides the greatest dosimetric and radiobiological benefits for liver tumors treated with SBRT, while AC offers comparable benefits for tumors <5 cm in diameter. Therefore, AC is recommended for liver tumors <5 cm in diameter undergoing SBRT.

## Data availability

Research data used during the current study are available from the corresponding author on reasonable request.

Received: 1 May 2025; Accepted: 8 September 2025

Published online: 14 October 2025

## References

1. Bray, F. et al. Global cancer statistics 2022: GLOBOCAN estimates of incidence and mortality worldwide for 36 cancers in 185 countries. *CA Cancer J. Clin.* **74**, 229–263. <https://doi.org/10.3322/caac.21834> (2024).
2. Tsimigras, D. I. et al. Liver metastases. *Nat. Rev. Dis. Primers.* **7**, 27. <https://doi.org/10.1038/s41572-021-00261-6> (2021).
3. Lau, W. Y. & Lai, E. C. Salvage surgery following downstaging of unresectable hepatocellular carcinoma—a strategy to increase resectability. *Ann. Surg. Oncol.* **14**, 3301–3309. <https://doi.org/10.1245/s10434-007-9549-7> (2007).
4. Tateishi, R. et al. Percutaneous radiofrequency ablation for hepatocellular carcinoma. An analysis of 1000 cases. *Cancer* **103**, 1201–1209. <https://doi.org/10.1002/cncr.20892> (2005).
5. Nakamura, A. et al. Analysis of dosimetric parameters associated with acute Gastrointestinal toxicity and upper Gastrointestinal bleeding in locally advanced pancreatic cancer patients treated with gemcitabine-based concurrent chemoradiotherapy. *Int. J. Radiat. Oncol. Biol. Phys.* **84**, 369–375. <https://doi.org/10.1016/j.ijrobp.2011.12.026> (2012).
6. Pan, C. C. et al. Radiation-associated liver injury. *Int. J. Radiat. Oncol. Biol. Phys.* **76**, 94–100. <https://doi.org/10.1016/j.ijrobp.2009.06.092> (2010).
7. Lee, J., Shin, I. S., Yoon, W. S., Koom, W. S. & Rim, C. H. Comparisons between radiofrequency ablation and stereotactic body radiotherapy for liver malignancies: Meta-analyses and a systematic review. *Radiother Oncol.* **145**, 63–70. <https://doi.org/10.1016/j.radonc.2019.12.004> (2020).
8. Thompson, R. et al. Outcomes of extra-cranial stereotactic body radiotherapy for metastatic colorectal cancer: dose and site of metastases matter. *Radiother Oncol.* **142**, 236–245. <https://doi.org/10.1016/j.radonc.2019.08.018> (2020).
9. Schaub, S. K. et al. Stereotactic body radiation therapy for hepatocellular carcinoma: current trends and controversies. *Technol. Cancer Res. Treat.* **17**. <https://doi.org/10.1177/1533033818790217> (2018).
10. Langen, K. M. & Jones, D. T. Organ motion and its management. *Int. J. Radiat. Oncol. Biol. Phys.* **50**, 265–278. [https://doi.org/10.1016/s0360-3016\(01\)01453-5](https://doi.org/10.1016/s0360-3016(01)01453-5) (2001).
11. Ten Haken, R. K., Balter, J. M., Marsh, L. H., Robertson, J. M. & Lawrence, T. S. Potential benefits of eliminating planning target volume expansions for patient breathing in the treatment of liver tumors. *Int. J. Radiat. Oncol. Biol. Phys.* **38**, 613–617. [https://doi.org/10.1016/s0360-3016\(97\)00009-6](https://doi.org/10.1016/s0360-3016(97)00009-6) (1997).
12. Gargett, M., Haddad, C., Kneebone, A., Booth, J. T. & Hardcastle, N. Clinical impact of removing respiratory motion during liver SABR. *Radiother Oncol.* **14**, 93. <https://doi.org/10.1186/s13014-019-1300-6> (2019).
13. Hardcastle, N. et al. Selection of motion management in liver stereotactic body radiotherapy and its impact on treatment time. *Phys. Imaging Radiat. Oncol.* **25**, 100407. <https://doi.org/10.1016/j.phro.2022.12.004> (2023).
14. Kilby, W., Dooley, J. R., Kuduvali, G., Sayeh, S. & Maurer, C. R. Jr. The cyberknife robotic radiosurgery system in 2010. *Technol. Cancer Res. Treat.* **9**, 433–452. <https://doi.org/10.1177/153303461000900502> (2010).
15. Lovelock, D. M., Zatzky, J., Goodman, K. & Yamada, Y. The effectiveness of a pneumatic compression belt in reducing respiratory motion of abdominal tumors in patients undergoing stereotactic body radiotherapy. *Technol. Cancer Res. Treat.* **13**, 259–267. <https://doi.org/10.7785/tcr.2012.500379> (2014).
16. West, K. et al. Evaluation of kidney motion with and without a pneumatic abdominal compression belt: considerations for stereotactic radiotherapy. *J. Med. Imaging Radiat. Oncol.* **62**, 128–132. <https://doi.org/10.1111/1754-9485.12681> (2018).
17. Eccles, C. L., Dawson, L. A., Moseley, J. L. & Brock, K. K. Interfraction liver shape variability and impact on GTV position during liver stereotactic radiotherapy using abdominal compression. *Int. J. Radiat. Oncol. Biol. Phys.* **80**, 938–946. <https://doi.org/10.1016/j.ijrobp.2010.08.003> (2011).
18. Ge, J., Santanam, L., Yang, D. & Parikh, P. J. Accuracy and consistency of respiratory gating in abdominal cancer patients. *Int. J. Radiat. Oncol. Biol. Phys.* **85**, 854–861. <https://doi.org/10.1016/j.ijrobp.2012.05.006> (2013).
19. Xi, M. et al. Dosimetric analysis of respiratory-gated radiotherapy for hepatocellular carcinoma. *Med. Dosim.* **36**, 213–218. <https://doi.org/10.1016/j.meddos.2010.03.006> (2011).
20. Dieterich, S., Green, O. & Booth, J. SBRT targets that move with respiration. *Phys. Med.* **56**, 19–24. <https://doi.org/10.1016/j.ejmp.2018.10.021> (2018).
21. Brandner, E. D., Chetty, I. J., Giaddui, T. G., Xiao, Y. & Huq, M. S. Motion management strategies and technical issues associated with stereotactic body radiotherapy of thoracic and upper abdominal tumors: A review from NRG oncology. *Med. Phys.* **44**, 2595–2612. <https://doi.org/10.1002/mp.12227> (2017).
22. Sharma, M. et al. A systematic review and meta-analysis of liver tumor position variability during SBRT using various motion management and IGRT strategies. *Radiother Oncol.* **166**, 195–202. <https://doi.org/10.1016/j.radonc.2021.11.022> (2022).
23. Hu, Y., Zhou, Y. K., Chen, Y. X., Shi, S. M. & Zeng, Z. C. 4D-CT scans reveal reduced magnitude of respiratory liver motion achieved by different abdominal compression plate positions in patients with intrahepatic tumors undergoing helical tomotherapy. *Med. Phys.* **43**, 4335. <https://doi.org/10.1118/1.4953190> (2016).
24. Hodapp, N. & [The, I. C. R. U. Report 83: prescribing, recording and reporting photon-beam intensity-modulated radiation therapy (IMRT)]. *Strahlenther Onkol.* **188**, 97–99. <https://doi.org/10.1007/s00066-011-0015-x> (2012).
25. Naumann, P. et al. Feasibility of optical Surface-Guidance for position verification and monitoring of stereotactic body radiotherapy in Deep-Inspiration Breath-Hold. *Front. Oncol.* **10**, 573279. <https://doi.org/10.3389/fonc.2020.573279> (2020).
26. Admiraal, M. A., Schuring, D. & Hurkmans, C. W. Dose calculations accounting for breathing motion in stereotactic lung radiotherapy based on 4D-CT and the internal target volume. *Radiother Oncol.* **86**, 55–60. <https://doi.org/10.1016/j.radonc.2007.11.022> (2008).
27. Ehler, E. D. & Tomé, W. A. Lung 4D-IMRT treatment planning: an evaluation of three methods applied to four-dimensional data sets. *Radiother Oncol.* **88**, 319–325. <https://doi.org/10.1016/j.radonc.2008.07.004> (2008).
28. Wang, P. M. et al. Stereotactic body radiation therapy in hepatocellular carcinoma: optimal treatment strategies based on liver segmentation and functional hepatic reserve. *Rep. Pract. Oncol. Radiother.* **20**, 417–424. <https://doi.org/10.1016/j.rpor.2015.03.005> (2015).

29. Méndez Romero, A. et al. Stereotactic body radiation therapy for primary and metastatic liver tumors: A single institution phase i-ii study. *Acta Oncol.* **45**, 831–837. <https://doi.org/10.1080/02841860600897934> (2006).
30. Wang, P. M. et al. Feasibility of stereotactic body radiation therapy with volumetric modulated Arc therapy and high intensity photon beams for hepatocellular carcinoma patients. *Radiat. Oncol.* **9**, 18. <https://doi.org/10.1186/1748-717x-9-18> (2014).
31. Timmerman, R. A. Story of hypofractionation and the table on the wall. *Int. J. Radiat. Oncol. Biol. Phys.* **112**, 4–21. <https://doi.org/10.1016/j.ijrobp.2021.09.027> (2022).
32. Niemierko, A. Reporting and analyzing dose distributions: a concept of equivalent uniform dose. *Med. Phys.* **24**, 103–110. <https://doi.org/10.1118/1.598063> (1997).
33. Gay, H. A. & Niemierko, A. A free program for calculating EUD-based NTCP and TCP in external beam radiotherapy. *Phys. Med.* **23**, 115–125. <https://doi.org/10.1016/j.ejmp.2007.07.001> (2007).
34. Gao, J. et al. Stereotactic body radiotherapy boost with the cyberknife for locally advanced cervical cancer: dosimetric analysis and potential clinical benefits. *Cancers* **14** <https://doi.org/10.3390/cancers14205166> (2022).
35. Liu, J., Wang, J. Z., Zhao, J. D., Xu, Z. Y. & Jiang, G. L. Use of combined maximum and minimum intensity projections to determine internal target volume in 4-dimensional CT scans for hepatic malignancies. *Radiat. Oncol.* **7**, 11. <https://doi.org/10.1186/1748-717x-7-11> (2012).
36. Koay, E. J., Owen, D. & Das, P. Radiation-Induced liver disease and modern radiotherapy. *Semin Radiat. Oncol.* **28**, 321–331. <https://doi.org/10.1016/j.semradonc.2018.06.007> (2018).
37. Hsieh, C. E. et al. Predictors of Radiation-Induced liver disease in Eastern and Western patients with hepatocellular carcinoma undergoing proton beam therapy. *Int. J. Radiat. Oncol. Biol. Phys.* **105**, 73–86. <https://doi.org/10.1016/j.ijrobp.2019.02.032> (2019).
38. Eccles, C. L. et al. Comparison of liver tumor motion with and without abdominal compression using cine-magnetic resonance imaging. *Int. J. Radiat. Oncol. Biol. Phys.* **79**, 602–608. <https://doi.org/10.1016/j.ijrobp.2010.04.028> (2011).
39. Heinzerling, J. H. et al. Four-dimensional computed tomography scan analysis of tumor and organ motion at varying levels of abdominal compression during stereotactic treatment of lung and liver. *Int. J. Radiat. Oncol. Biol. Phys.* **70**, 1571–1578. <https://doi.org/10.1016/j.ijrobp.2007.12.023> (2008).
40. Gabryś, D., Kulik, R., Trela, K. & Ślosarek, K. Dosimetric comparison of liver tumour radiotherapy in all respiratory phases and in one phase using 4DCT. *Radiation Oncol.* **100**, 360–364. <https://doi.org/10.1016/j.radonc.2011.09.006> (2011).
41. Emami, B. et al. Tolerance of normal tissue to therapeutic irradiation. *Int. J. Radiat. Oncol. Biol. Phys.* **21**, 109–122. [https://doi.org/10.1016/0360-3016\(91\)90171-y](https://doi.org/10.1016/0360-3016(91)90171-y) (1991).
42. Chang, J. H. et al. A simple program for utilising biological modelling in radiotherapy plan evaluation. *Phys. Med.* **32**, RADBIOMOD, 248–254. <https://doi.org/10.1016/j.ejmp.2015.10.091> (2016).
43. Balasubramanian, S. & Shobana, M. K. A dosimetric and Radiobiological comparison of intensity modulated radiotherapy, volumetric modulated Arc therapy and helical tomotherapy planning techniques in synchronous bilateral breast cancer. *Asian Pac. J. Cancer Prev.* **23**, 4233–4241. <https://doi.org/10.31557/apjcp.2022.23.12.4233> (2022).
44. Balasubramanian, S. & Shobana, M. K. Pediatric craniospinal Irradiation - The implementation and use of normal tissue complication probability in comparing photon versus proton planning. *J. Med. Phys.* **46**, 244–252. [https://doi.org/10.4103/jmp.jm\\_p\\_75\\_21](https://doi.org/10.4103/jmp.jm_p_75_21) (2021).
45. Vaithianathan, H. & Harris, B. Transmission study of the abdominal compression plate (BodyFIX diaphragm Control) for abdominal and stereotactic body radiotherapy. *J. Appl. Clin. Med. Phys.* **22**, 232–241. <https://doi.org/10.1002/acm2.13373> (2021).

## Author contributions

Z.H.X., J.X.G., T.X.: Conceptualization, Investigation, Formal analysis, Methodology, Writing - original draft. H.H.L., Q.H.C.: Formal analysis, Data curation, Visualization. J.S.L., M.Y.H.: Software, Resources, Validation. X.D.W.: Project administration, Supervision. Y.G.C.: Writing - review & editing, Funding acquisition, Conceptualization. All authors read and approved the final version of the manuscript.

## Funding

This research was funded by Natural Science Foundation of Fujian Province (2021J01740); Joint Funds for the Innovation of Science and Technology, Fujian Province (2023Y9136) and Subsidy Funds for the health, Fujian Provincial Department of Finance (2023CZ007).

## Declarations

## Ethics approval and consent to participate

The study was approved by the Research Ethics Committee of Fujian Medical University Union Hospital (Fuzhou, China; approval no. 2024ky017).

## Competing interests

The authors declare no competing interests.

## Additional information

**Correspondence** and requests for materials should be addressed to X.W. or Y.C.

**Reprints and permissions information** is available at [www.nature.com/reprints](http://www.nature.com/reprints).

**Publisher's note** Springer Nature remains neutral with regard to jurisdictional claims in published maps and institutional affiliations.

**Open Access** This article is licensed under a Creative Commons Attribution-NonCommercial-NoDerivatives 4.0 International License, which permits any non-commercial use, sharing, distribution and reproduction in any medium or format, as long as you give appropriate credit to the original author(s) and the source, provide a link to the Creative Commons licence, and indicate if you modified the licensed material. You do not have permission under this licence to share adapted material derived from this article or parts of it. The images or other third party material in this article are included in the article's Creative Commons licence, unless indicated otherwise in a credit line to the material. If material is not included in the article's Creative Commons licence and your intended use is not permitted by statutory regulation or exceeds the permitted use, you will need to obtain permission directly from the copyright holder. To view a copy of this licence, visit <http://creativecommons.org/licenses/by-nc-nd/4.0/>.

© The Author(s) 2025